

# My Thesis Title

Philip Gemmell  
Oriel College



Computational Biology Research Group  
Computing Laboratory  
University of Oxford

**Define Term**

This thesis is submitted to the Computing Laboratory, University of Oxford, for the degree of Doctor of Philosophy. This thesis is entirely my own work, and, except where otherwise indicated, describes my own research.

Philip Gemmell  
Oriel College

Doctor of Philosophy  
Define Term

# **My Thesis Title**

## **Abstract**

This thesis describes stuff aplenty.

# Contents

---

<b>1</b>	<b>Introduction</b>	<b>1</b>
<b>2</b>	<b>Literature Review</b>	<b>2</b>
2.1	Cardiac Physiology . . . . .	3
2.2	Computational Cell Models . . . . .	14
2.3	Variation . . . . .	17
2.4	Ischæmia . . . . .	17
<b>A</b>	<b>Diffusion</b>	<b>18</b>
A.1	Simple Diffusion . . . . .	18
A.2	Facilitated Diffusion, Michaelis-Menten Kinetics . . . . .	19
A.3	Electrodiffusion . . . . .	20

# List of Figures

---

2.1	Structure of the mammalian heart . . . . .	3
2.2	Structure of myocardial sheets and fibres . . . . .	4
2.3	Pattern of electrical activation in the heart . . . . .	6
2.4	Schematic of a cardiac AP . . . . .	8

## List of Tables

---

## Acknowledgements

This thesis is the culmination of many year's work and would not have been possible without the help and support of many people.

First and foremost I would like to thank my supervisor, Dr X, for his mindless support and useless proof-reading. Blah, gibber ...

Many of the ideas presented are the outcome of discussions with members of the Computational Biology Group and beyond. In particular I owe much to X and Y who ...

My research was funded by a ...

Throughout this year I have enjoyed the unfailing support of my pet hamster.

## *Notation & Nomenclature*

---

AP	Action Potential
AP <sub>RMS</sub>	Root mean square difference between ‘test’ and ‘training’ data for $V_m$ data
APD <sub><math>x</math></sub>	Action potential duration to $x\%$ repolarisation
[Ca <sup>2+</sup> ] <sub>i</sub>	Free cytosolic Ca <sup>2+</sup> concentration
$g_X$	Maximum conductance for current $X$
$I_{Ca,L}$	L-type Ca <sup>2+</sup> current
$I_{K1}$	Inward rectifying K <sup>+</sup> current
$I_{Kr}$	Rapidly delayed rectifier K <sup>+</sup> current
$I_{Ks}$	Slowly delayed rectifier K <sup>+</sup> current
$I_{Na}$	Na <sup>+</sup> current
$I_{NaCa}$	Na <sup>+</sup> -Ca <sup>2+</sup> exchanger current
$I_{NaK}$	Na <sup>+</sup> -K <sup>+</sup> pump current
$I_{stim}$	Stimulus current
$I_{to}$	K <sup>+</sup> transient outward current
$I_{to,f}$	Fast K <sup>+</sup> transient outward current
$I_{to,s}$	Slow K <sup>+</sup> transient outward current
$V_m$	Membrane potential
$\Delta[Ca^{2+}]_i$	Difference between systolic [Ca <sup>2+</sup> ] <sub>i</sub> and diastolic [Ca <sup>2+</sup> ] <sub>i</sub>

# INTRODUCTION

# 1

This will be the introduction.



# LITERATURE REVIEW



*There are more things in heaven and earth, Horatio,*

*Than are dreamt of in your philosophy.*

*(Hamlet, Act 1, Scene 5)*

---

*In this section, the relevant background information is given. This starts with a brief outline of the function and structure of the heart, ranging from the high order organisation of the heart into functional compartments, down to the cellular level. Further details are then given on the physiological aspects of some of the subcellular components of cardiac tissue. The evolution of computational models to describe the electrical activity of the heart is charted briefly, with special attention given to models specifically used in this thesis. Variation is then described, both in experimental and physiological measurements, and how this variation has been addressed in computational models. Then the pathological condition of ischæmia will be described, and the computational efforts to model this outlined.*

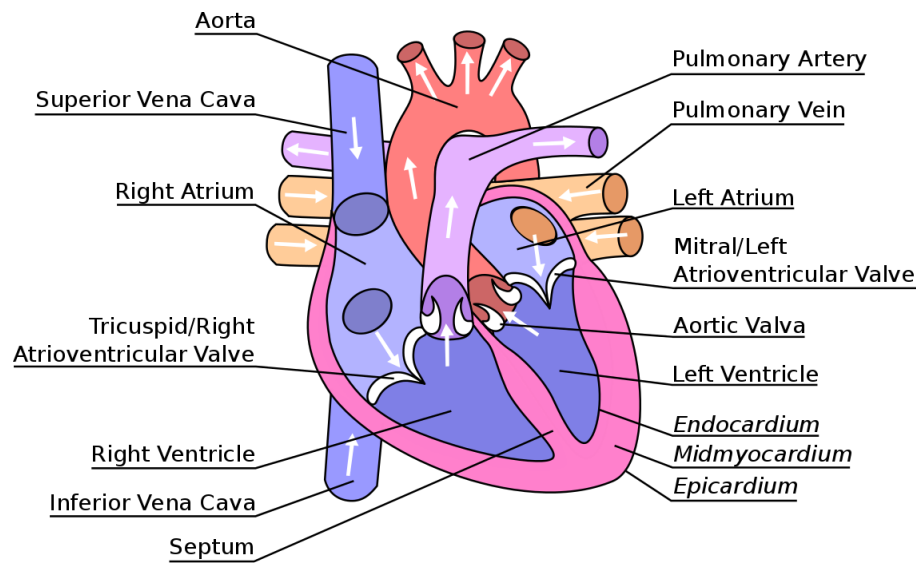


**Figure 2.1:** *Diagram of the longitudinal cross-section of a mammalian heart. The direction of blood flow is shown by white arrows, and all major structural components are labelled.*

## 2.1 Cardiac Physiology

At the most general level, the heart serves as a pump to transport blood around the body to deliver nutrients and remove waste products. It does this by rhythmic, organised contraction—the rate of this contraction varies depending on species, age, condition of the heart and the activity being undertaken by the organism.

### 2.1.1 Structure of the Mammalian Heart

Fig. 2.1 shows the anatomical structure of the mammalian heart—while the size obviously varies widely between mammals, the overall architecture remains constant. It is split into two halves, left and right, by a muscular wall called the *septum*, and then further subdivided into two chambers, the larger, lower chamber being a *ventricle*, and the smaller, upper chamber called an *atrium*.

The passage of blood through the heart follows thus: firstly, deoxygenated blood from the body enters the heart via the superior and inferior/posterior *vena cava*, with superior and inferior representing whether the blood comes from the upper or lower half of the body respectively. Via this channel, it enters the *right atrium*. Passing through the *tricuspid*

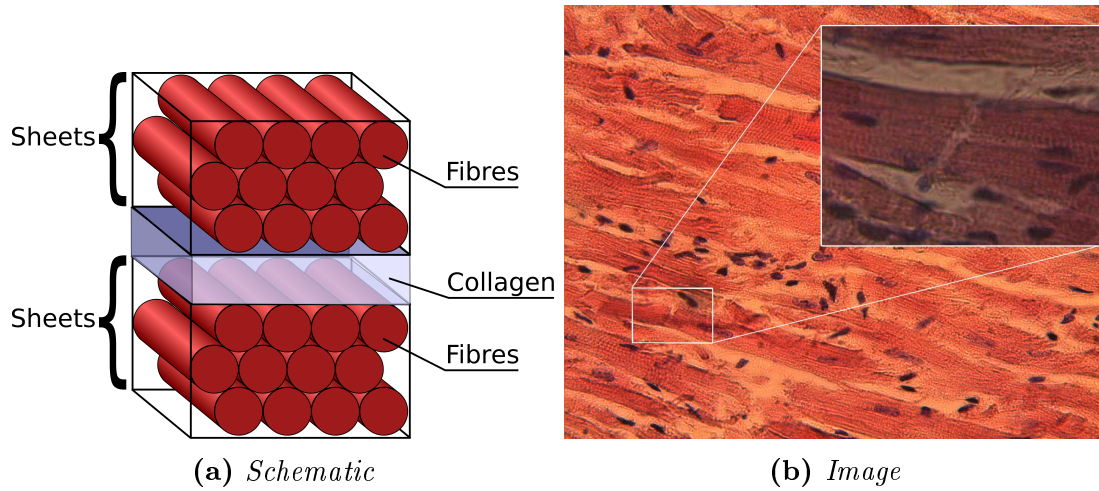


**Figure 2.2:** (2.2a) Schematic of the structure of myocardial sheets and fibres. (2.2b) Image of cardiomyocytes demonstrating the interconnected nature of the individual myocytes into fibres.

*valve* (also known as the right atrioventricular valve), the blood enters the *right ventricle*, where it is then pumped via the *pulmonary artery* to the lungs, where it is oxygenated. The blood returns to the heart via the *pulmonary vein*, entering the *left atrium*, before moving through the *mitral valve* (also known as the left atrioventricular valve) into the *left ventricle*. The blood is then pumped via the *aorta* to the rest of the body. The valves in the heart serve to ensure the flow of blood is always in the correct direction.

The walls of the heart are mostly composed of muscular tissue known as *myocardium*. The thickness of the myocardium is not constant throughout the heart, being thickest in the left ventricle, which requires the greatest force of contraction to pump the blood from the heart to the rest of the body. The myocardium can be split into three different regimes, as labelled in italics in Fig. 2.1: the *epicardium* is the outermost layer of the myocardium, the *midmyocardium* is the middle layer, and the *endocardium* is the innermost layer. The cells composing these different layers possess different electrophysiological properties; the differences, and the consequences, will be expanded upon in §2.1.2.

The structure within the myocardium is shown in Fig. 2.2a: it is composed of a series of sheets of tissue separated by collagen. The myocytes themselves lie longitudinally in these sheets to form fibres, with myocytes in the fibre direction connected to each other by intercalated discs (as opposed to skeletal muscle, which is composed of multinucleated

fibres); this structure is seen in Fig. 2.2b. One attribute of these discs is the presence of *gap junctions*, which serve to electrically couple the myocytes by allowing ion flow between the two neighbouring myocytes in the fibre direction. This arrangement of the myocytes into electrically coupled fibres allows for coordinated contraction, and the fibrous structure allows the heart to twist as it contracts, leading to a more efficient pumping mechanism.

The conduction pattern of the heart is key to the effective pumping mechanism—by controlling the sequence of electrical events in the heart, the sequence of conduction is similarly controlled. An outline of the conduction pattern of the heart is shown in Fig. 2.3. The sequence of activation starts amongst a group of self-excitatory cells at the top of the right atrium, called the *sinoatrial node*. The action potential wave spreads from this node, causing the atrium to contract, before it reaches the *atrioventricular node*—this is the only pathway for electrical excitation to pass from the atria to the ventricles. From the atrioventricular node, the excitation wave passes to the *Bundle of His*, which conducts the electrical stimulus via the left and right bundle branches into the *Purkinje system* near the bottom of the heart, which transmits the stimulus to the ventricular surface; as the stimulus has thus been transmitted directly from the atria to the bottom of the ventricles, the excitation wave thus spreads upwards through the ventricles, allowing the ventricles to contract from the bottom up as required.

### 2.1.2 Electrophysiological Properties of Cardiomyocytes

As previously stated, the main rôle of the heart is to serve as a pump to circulate the blood around the body. To do this effectively, it requires coordinated contraction, and this is achieved through the use of coupling the electrical activity of the heart of the mechanical activity (the details of this mechanism will be expanded upon in §2.1.2).

Physically, cardiomyocytes are typically  $10 - 20\mu\text{m}$  in diameter, and  $50 - 100\mu\text{m}$  in length. They are cells bound by a lipid bilayer membrane, separating intracellular space

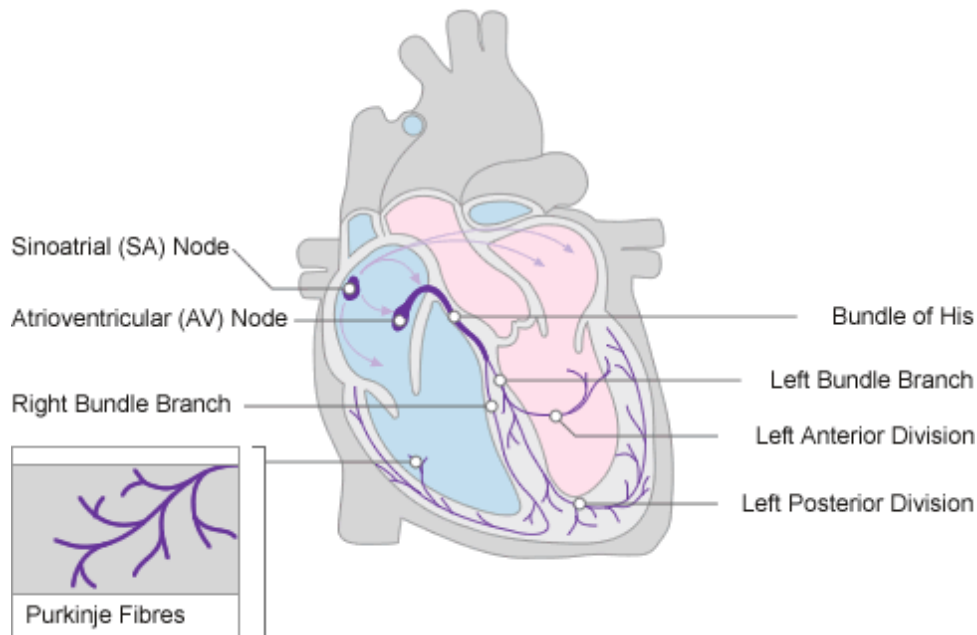


**Figure 2.3:** Schematic outline of the sequence of electrical activation in the mammalian heart. Image originally downloaded from [www.nottingham.ac.uk](http://www.nottingham.ac.uk) on 10th December 2012.

(containing the cytoplasm, nuclei and other organelles) from the extracellular space. The intracellular space has a very different composition to the extracellular space, with the intracellular space containing a high and low concentration of potassium ( $K^+$ ) and sodium ( $Na^+$ ) ions respectively; the reverse is true for the extracellular space. These concentration differences are the main reason behind their being a potential difference set up across the cell membrane, referred to as the *membrane potential* ( $V_m$ ). At rest, due to the high  $K^+$  and low  $Na^+$  in the cell, this potential is negative, though the magnitude varies depending upon the location in the heart; a cardiomyocyte in the ventricles typically has a resting potential ( $V_{rest}$ ) of about  $-80mV$ , while the sinoatrial node has a resting potential of between  $-50$  and  $-60mV$ .

Embedded within the bilayer are various membrane-bound proteins which serve to transport ions across the membrane, allowing the membrane to be selectively permeable to particular ions, and allowing regulation of this permeability as required. These transporters can be classed as either *channels* (allow ions to move according to their electrochemical gradient), *pumps* (translocate ions in the opposite direction to their electrochemical gradient by the use of energy) or *exchangers* (translocates a number of ions of one type across

the membrane in ‘exchange’ for a number of ions of another type). Most of these transporters are ion-specific, though some are not exclusively selective. Most of these channels are also controlled by, amongst other things, the membrane potential itself (1). The membrane potential causes a conformational change in the ion channel protein, causing it to ‘open’ or ‘close’, that is to allow ions to be conducted through it or not.

These ion channels are discrete molecular entities, and thus the conformational changes that lead to their open/close state are stochastic; the effects of this stochasticity are discussed in greater detail in §2.3. However, each type of ion channel possesses its own range of attributes, such as the time it takes to inactivate, the time it takes to reactivate, its permeability to different types of ions, and its susceptibility to other gating factors. Comprehensive summaries of the properties of ion channels is given in Carmeliet and Vereecke (3), Roden et al. (12).

Electrically, the heart can be modelled with great success as an analogue to an electrical circuit (3), where the lipid bilayer is represented as a capacitor, and the various ion channels and transporters that span the membrane are represented as resistors, which change their ‘resistance’ depending on their state. By altering the resistance of these channels, ion flow across the membrane is permitted via an ionic current. It is a point of nomenclature that an ‘inward’ current represents the movement of positive ions from the extracellular to the intracellular space, and an ‘outward’ current is the reverse. This definition is based on the movement of electrical charge, and not on the movement of ion flow. This is subtly different to the definition of an inward or outward rectifier current, where an inward rectifier current passes current more easily inward than outward, and vice versa for an outward rectifier current.

The changes in internal/external ion concentrations which result from these currents changes  $V_m$ . The cyclic, periodic change in membrane potential is referred to as the *action potential* (AP). An example of an action potential, showing the different ‘phases’, is shown in Fig. 2.4.

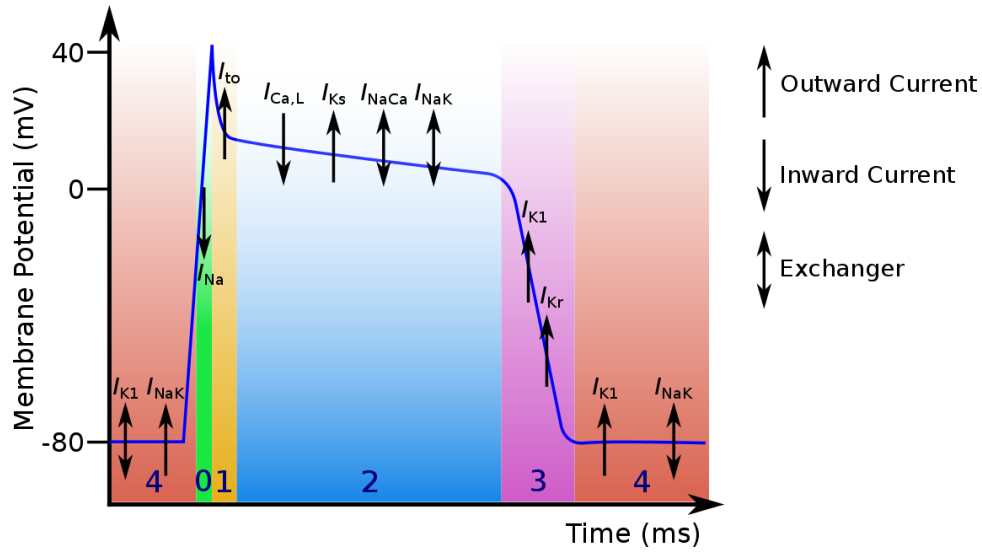


**Figure 2.4:** Schematic of a ventricular cardiac AP, with the different ‘phases’ of the AP shown, and which key currents are involved in each phase. Upward arrows represent outward currents, inward currents represent inward currents, and double arrows represent exchangers, i.e., where current moves in both an inward and outward direction.

The AP is considered to consist of 5 different phases, outlined below. The important currents in each phase are mentioned, and greater details are given for a number of these current in §2.1.2.

**Phase 4:** The resting phase. For ventricular and atrial cardiomyocytes, this phase is marked by a relatively constant value for  $V_m$ . The negative resting potential is largely achieved by the inwardly rectifying potassium current ( $I_{K1}$ ) remaining open during this phase. For pacemaker cells,  $I_{K1}$  is absent, and thus the resting phase is actually a period of slow depolarisation, until  $V_m$  reaches the threshold value for phase 0. There is also an inward current due to the  $\text{Na}^+$ - $\text{Ca}^{2+}$  exchanger current ( $I_{\text{NaCa}}$ ), which moves 3  $\text{Na}^+$  ions into the cell and one  $\text{Ca}^{2+}$  ion out at the resting potential.

**Phase 0:** Period of rapid depolarisation that marks the start of the AP. It is initiated by  $V_m$  reaching a threshold value which causes the  $I_{\text{Na}}$  current to activate, causing a rapid influx of  $\text{Na}^+$  into the cell. The direction of  $I_{\text{NaCa}}$  reverses, and this newly outward current brings in  $\text{Ca}^{2+}$  and removes  $\text{Na}^+$ .

**Phase 1:** Transient repolarisation. The  $\text{Na}^+$  channels rapidly deactivate, and the ac-

tivation of the transient  $K^+$  outward current ( $I_{to}$ , occasionally referred to as  $I_{to1}$ ) results in a period of rapid, partial repolarisation. There may also be a contribution from a  $Ca^{2+}$ -activated  $Cl^-$  ( $I_{CaCl}$ , or  $I_{to2}$ ). Depending on the strength of this current, this repolarisation may be to the extent that there is a ‘notch’ in the AP. For example, there is a notch in the AP for ventricular epicardial cells, but no notch for ventricular endocardial cells. The characteristics of this phase are also species-dependent (2).

**Phase 2:** Plateau phase. The membrane potential is sustained at a relatively constant level by a balance of calcium ( $Ca^{2+}$ ) influx via the L-type calcium current ( $I_{Ca,L}$ ), and potassium efflux, through the rectifier  $K^+$  currents (rapid,  $I_{Kr}$ , and slow,  $I_{Ks}$ ). Despite being a rapidly activated current,  $I_{Kr}$  does not carry large current early during this phase, but only peaks at the end.  $I_{K1}$  shows a dramatic fall in conductance during this phase. While most  $I_{Na}$  is inactivated during phase 1, there is a small contribution from  $I_{Na}$  when  $V_m$  is in the limited range where activation and inactivation both occur. Late during phase 2, due to the increase in  $[Ca^{2+}]_i$ , the reversal potential for  $I_{NaCa}$  increases to a value greater than  $V_m$ , and thus  $I_{NaCa}$  returns to being an inward current.

**Phase 3:** Repolarisation. The L-type  $Ca^{2+}$  current channels close, while the  $I_{Ks}$  channels remain open, allowing continuing  $K^+$  efflux resulting in a repolarisation of the cell to the original resting potential.  $I_{K1}$  opens during this phase, to remain open during phase 4 to maintain a steady resting potential.

It should be noted that the above description of which currents act during which phase is only an outline. While the upstroke of the AP is due mostly to the action of  $I_{Na}$  and the associated rapid influx of  $Na^+$  ions into the cell, causing the rapid depolarisation, the remaining phases of the AP are more complex, and the failure or part failure of any individual component of the cell mechanism does not necessarily lead to the failure of the whole system. This pseudo-redundancy was first termed *repolarisation reserve* in



Roden (11), and was demonstrated experimentally in Varró et al. (18). It is essentially the concept that a delay in repolarisation function caused by a reduction or loss of function in one repolarising current can be recovered by increased action of an alternative repolarising current. Most often, this term is applied to  $K^+$  channels, and specifically for the interaction between  $I_{Kr}$  and  $I_{Ks}$  (20). Several currents are of noted for their rôle in maintaining the repolarisation reserve of the cell, some of which have already been mentioned:  $I_{Kr}$ ,  $I_{Ks}$ ,  $I_{K1}$ ,  $I_{to}$ ,  $I_{Ca,L}$ ,  $I_{Na}$  (17). The repolarisation reserve is not constant, but rather is dynamic with pacing rate, and variable between species and tissues within the heart (2).

### **Ion Channel Dynamics**

$I_{Kr}$ , as the name implies, is the more rapidly activating of the two rectifier  $K^+$  currents ( $\tau \sim 40\text{ms}$  at  $+30\text{mV}$ ), and rapidly activates once  $V_m$  increases above  $-30\text{mV}$ . However, the channel inactivates even more rapidly in a process that precedes voltage-dependent inactivation (17, 15, 2). Due to this,  $I_{Kr}$  channels are largely closed during the plateau phase of the AP, only reopening when  $V_m$  returns to about  $0\text{mV}$ . The transient nature of the current is due to its rapid recovery from inactivation, and subsequent slow deactivation. At slow rates, the contribution of  $I_{Kr}$  diminishes further, resulting in a positive feedback loop regarding AP duration (APD) lengthening (the same is observed for  $I_{K1}$ ) (19). This same vulnerability of the repolarisation is evident when depolarising factors (*e.g.*,  $I_{Na}$ ,  $I_{Ca,L}$ ) are augmented or repolarising factors (*e.g.*,  $I_{Ks}$ ,  $I_{K1}$ ) diminished.

If its function is impaired substantially in some way, APD is significantly prolonged by both direct measurements and QT interval measurements in electrocardiograms (ECGs) (the QT interval serves as a marker for the time taken for ventricular depolarisation and repolarisation in a clinical setting), suggesting especial importance in cellular repolarisation (18, 10, 9). When  $I_{Kr}$  is only impaired in a minor way, APD may not necessarily increase due to the action of the repolarisation reserve.  $I_{Kr}$  is due to a channel encoded by the human ether-à-go-go related gene (HERG), and is known for being its susceptibility

to the effects of drug block, making it of key pharmacological importance (16, 7).

$I_{Ks}$  takes longer to activate than its partner (500-1000ms at plateau phase), and deactivates rapidly at negative  $V_m$  (9, 17). It carries a slowly rising current over the duration of the plateau phase. At rapid pacing rates, the current carried by the  $I_{Ks}$  channel increases—this is thought to be due to the kinetics of the channel, with an ‘inactivated’ state being intermediate between the open and closed state. At rapid pacing rates, there is less time to transition fully to the closed state, and thus there is a greater proportion of  $I_{Ks}$  channels available for immediate opening (14).

Drug block of  $I_{Ks}$  does cause AP prolongation, but not to the same extent as  $I_{Kr}$ ; while direct measurements show a slight increase in APD, there is very little or no change in QT intervals ECG measurements (18, 10, 9). This implies that its amplitude, compared to that of  $I_{Kr}$ , during a typical AP is small—this has been confirmed experimentally under normal conditions (17). Combined with its slow activation, there is thus relatively little  $I_{Ks}$  active during the AP (9). However, its long activation time also means the effect of  $I_{Ks}$  block is more pronounced APD is prolonged, due to (i) the net outward current at long pacing rates is smaller, so the fractional effect of  $I_{Ks}$  is greater, and (ii) more channels are activated during a long AP (2). Due to this action, and the response of  $I_{Ks}$  to sympathetic stimulation, the current provides a negative feedback for APD prolongation, acting to curtail the increased action of  $I_{Ca,L}$  that occurs at longer pacing rates. Thus, while under ‘normal’ circumstances  $I_{Ks}$  has limited effect on the repolarisation reserve of the cell, it acts as an effective buffer when APD is longer than normal.

The transmural differences in the expression of  $I_{Ks}$  is a large reason behind the transmural variation of APD, and also explains why  $I_{Kr}$  block can have a greater or lesser effect, depending on the abundance of the compensatory effect of  $I_{Ks}$  (16, 2). The density of  $I_{Ks}$  channels has also been shown to increase in response to sustained  $I_{Kr}$  block, demonstrating its importance to the repolarisation reserve (20).

$I_{K1}$  is a strongly inwardly rectifying  $K^+$  current, which means that when  $V_m$  is greater

than  $-30\text{mV}$ , the channel is inactivated. Thus it plays a negligible rôle during the plateau phase of the AP, but has a self-reinforcing role in the repolarisation of the cell once  $V_m$  decreases to the extent that  $I_{K1}$  can be activated. It should be noted that this is not a voltage-dependent activation, but is based on an unblocking of the channel: when  $V_m > -30\text{mV}$ , the channel is blocked by  $\text{Mg}^{2+}$  and polyamines which enter the channel from the intracellular side in a voltage-dependent manner. As the current is fully open at  $V_{\text{rest}}$ , it resists depolarisation caused by either increased pacemaker activity, or  $\text{Ca}^{2+}$  overload-related delayed afterdepolarisations (DADs). Consequently,  $I_{K1}$  may be considered to play an unusual rôle in the repolarisation reserve, and impairment of its function could lead to proarrhythmic effects by making the cell more susceptible to extrasystoles.

$I_{\text{to}}$  is actually composed of two separate currents, a rapidly recovering component ( $I_{\text{to,f}}$ ) and a slowly recovering component ( $I_{\text{to,s}}$ ). As a combined unit, it both activates and inactivates rapidly for  $V_m > -20\text{mV}$ , and is of greatest importance during the phase 1 repolarisation. As such, it is believed to have little influence directly on the end repolarisation of the cell, but due to its early role, and its consequent effect on the plateau potential, it is believed to have influence on subsequent currents, which lead to great indirect influence.  $I_{\text{to}}$  is also known for its transmural variation, being greater in epicardial than endocardial tissue.

$I_{\text{NaK}}$  is caused due to the  $\text{Na}^+\text{-K}^+$  pump, which is an electrogenic exchanger, moving 3  $\text{Na}^+$  ions out of the cell in exchange for 2  $\text{K}^+$  ions. It thus works to maintain the concentration gradients and the resting membrane potential, and provides an outward current in support of the repolarisation reserve. It is, however, sensitive to intracellular  $\text{Na}^+$  concentration ( $[\text{Na}^+]_{\text{i}}$ ), and consequently to the rate of stimulation.

The influence of  $I_{\text{Ca,L}}$  on the repolarisation of the cell is complex due to its complicated inactivation. It inactivates due to voltage slowly, and thus the main reason for its inactivation is due to  $\text{Ca}^{2+}$ -induced inactivation, and is thus in response to local  $\text{Ca}^{2+}$

concentration, which is dynamically changing during the plateau phase. This inactivation is modulated via a protein called calmodulin, and thus can be modulated further. If the AP is extended during the range of activation/inactivation for  $I_{Ca,L}$ , some  $I_{Ca,L}$  channels may reactivate. This resurgence of the inward current can lead to secondary depolarisations or early after-depolarisations (EADs) (2).

If  $I_{Ca,L}$  (or  $I_{Na}$ ) are augmented and have their activity increased, this serves to make the plateau potential more positive. While at first glance this may indicate that AP may lengthen, it is rather the case that this may serve to enhance activation of outward  $K^+$  currents, thus shortening APD.

The  $Na^+$ - $Ca^{2+}$  exchange current ( $I_{NaCa}$ , also referred to as  $I_{NCX}$ ), like  $I_{NaCa}$ , is an electrogenic exchanger, this time exchanging 3  $Na^+$  ions for one  $Ca^{2+}$  ion. By this process, it is, with the SERCA pump, largely responsible for restoring the low cytosolic  $Ca^{2+}$  concentration during diastole. It depends strongly on  $V_m$  and  $[Ca^{2+}]_i$ , and thus its magnitude during the AP is difficult to estimate (a problem compounded by the lack a specific inhibitor for the current). It is an outward current at the start of the AP, when  $V_m$  and  $[Ca^{2+}]_i$  are both low, but then changes to an inward current during the late plateau phase. Due to its sensitivity to  $[Ca^{2+}]_i$ , in times of  $Ca^{2+}$ -overload  $I_{NaCa}$  can provide a depolarising current, thus increasing the likelihood of DADs and EADs. The density of  $I_{Na}$  is also known to depend heavily on  $[Ca^{2+}]_i$ , decreasing when  $[Ca^{2+}]_i$  is high; the gating of the channel is not affected.

### Excitation-Contraction Coupling

Arguably, the complex electrical activity of the AP just described exists for the sole purpose of ensuring the heart acts as an effective mechanical pump. As such, the linking of the electrical activity of the heart to its mechanical contraction is vital, as is referred to as *excitation-contraction coupling*. What follows is a brief summary of the mechanism of this link (the reverse side of this mechanism, termed mechanoelectric feedback, shall

not be discussed here).

For this discussion, the cell may be decomposed into units called calcium release units (CRUs), also known as dyads (4). These CRUs are spread roughly evenly throughout the cell to allow for a uniform action throughout—the number of CRUs in the cell has been estimated to be between 10,000 and 100,000 (4, 6). Anatomically, the CRU may be considered to be a section of the cell containing a section of the cell membrane, with some L-type  $\text{Ca}^{2+}$  channels, and a section of the sarcoplasmic reticulum (SR). The primary rôle of the SR is to sequester and release  $\text{Ca}^{2+}$  via ryanodine receptors (RyRs) when the required stimulus is given. This stimulus is the rise in local concentration of  $\text{Ca}^{2+}$  precipitated by the opening of the L-type  $\text{Ca}^{2+}$  current channels, and is termed *calcium-induced calcium release*. The result is that a great deal of  $\text{Ca}^{2+}$  is released into the cytosol of the cell during phase 2 of the AP. The reason this is vital for ECC is due to the interaction between  $\text{Ca}^{2+}$  and the contractile units of the cell, called the sarcomere. When the cytosolic concentration of  $\text{Ca}^{2+}$  ( $[\text{Ca}^{2+}]_i$ ) rises, the free  $\text{Ca}^{2+}$  binds to a part of the contractile machinisms of the cell, which then removes the inhibition between the two critical contractile parts of the mechanism, allowing contraction to take place. Subsequently, the  $\text{Ca}^{2+}$  released from the SR is recovered by the sarco/endoplasmic reticulum  $\text{Ca}^{2+}$ -ATPase pumps (5).

## 2.2 Computational Cell Models

It is often not practicable to test hypotheses in full experimental conditions. In such times, computational/mathematical models have become of increasing importance in recent years, as they have developed from their original humble origins. Depending on the requirements of the model, great advances have been made in accurately modelling individual ion channels, assessing the importance of stochasticity, to probing the interplay between systems and levels in complicated simulations. What follows is a brief background on the evolution and development of computational cell models from their early

days in §2.2.1, and then a summary of some of the key concepts that are of use in these models in §2.2.2.

### 2.2.1 Development

The precursor to all computational models of cardiac cells was the model developed in Hodgkin and Huxley (8). This model described the electrical activity of a giant squid axon. It described the ionic currents required to explain the change in membrane potential, using a model for each current of a series of activation and inactivation gating variables (details given in §2.2.2).

### 2.2.2 Key Concepts

In biophysically detailed models of electrically excitable cells, all ionic currents can be modelled according to:

$$I_X = g_X(\mathbf{x})(V_m - E_X), \quad (2.1)$$

where  $I_X$  represents the ionic current being modelled,  $g_X(\mathbf{x})$  represents the conductance of the channel and  $E_X$  represents the reversal potential of the cell, which is the potential at which there is no net ion flow through the channel, *i.e.*, there will be no ionic current. The general form of  $E_X$  is explained in §2.2.2.  $g_X(\mathbf{x})$  is current-dependent variable, and can be modelled as varying with time, voltage, extra-/intracellular ion concentration, etc..

#### Nernst Potential

Of key importance in mathematical modelling of electrically active cells is the *Nernst equation*. A full derivation is given in the appendix, but the key result is thus:

$$E_X = \frac{RT}{z_X F} \ln \frac{[X]_o}{[X]_i} \quad (2.2)$$

In the above equation,  $R$  represents the gas constant,  $z_X$  represents the valence of ion  $X$ ,  $F$  represents the Faraday constant, and  $[X]_o$  and  $[X]_i$  represent the extracellular and

intracellular concentrations of  $X$  respectively. The quantity of interest,  $E_X$  is the *Nernst potential* or *reversal potential*, and represents the value of  $V_m$  required to maintain the intra-/extracellular concentration ratio constant, *i.e.*, to make the net ionic flux across the cell membrane zero.

When a channel is entirely selective, the reversal potential (which can now be thought of as the potential at which there will be no net flux of ions) is given by the Nernst equation for the specific ion. However, some ion channels are permeable to more than one type of ion, in which case their reversal potential for channel  $\alpha$  is given by the *Goldman-Hodgkin-Katz equation*:

$$E_\alpha = \frac{RT}{F} \ln \frac{\sum_i^N P_{A_i^+} [A_i^+]_o + \sum_j^M P_{B_j^-} [B_j^-]_i}{\sum_i^N P_{A_i^+} [A_i^+]_i + \sum_j^M P_{B_j^-} [B_j^-]_o} \quad (2.3)$$

The above equation describes the situation for  $N$  different monovalent positive ionic species and  $M$  monovalent negative ionic species; different valencies complicate matters further. In it,  $E_\alpha$  represents the reversal potential for the channel, *i.e.*, the potential at which, with the given ion concentrations, no net electric flow will occur. The permeability of the membrane is given by  $P_X$ ; as with the concentrations, the terms have been split into positive ( $A_i^+$ ) and negative ( $B_j^-$ ) ionic terms.

### Hodgkin-Huxley Current

As previously stated, the seminal work presented in Hodgkin and Huxley (8) modelled currents as being composed of one of more activation/inactivation gates. As such, the current conductance can be modelled according to

$$g_X = \overline{g_X} m^a h^b, \quad (2.4)$$

where  $\overline{g_X}$  represents the maximum conductance through the channel,  $a$  and  $b$  are constants,  $m$  represents the activation gate and  $h$  the inactivation gate. These vary according to the following pattern (the same is true for  $h$ ):

$$\frac{dm}{dt} = \alpha_m(1 - m) - \beta_m, \quad (2.5)$$

where  $\alpha_m$  and  $\beta_m$  are functions of  $V_m$ . It can be noted that this can be expressed alternatively:

$$\frac{dm}{dt} = \frac{m_\infty - m}{\tau_m} \quad (2.6)$$

where  $m_\infty = \alpha_m / (\alpha_m + \beta_m)$  and  $\tau_m = 1 / (\alpha_m + \beta_m)$ .

At a basic level, in mathematical models of ion channel currents, it is assumed that, instantaneously, they behave like Ohmic resistors, *i.e.*

## 2.3 Variation

### 2.3.1 Experimental & Physiological Variation

### 2.3.2 Computational Modelling of Variation

## 2.4 Ischæmia

Despite what would be expected from the Nernst equation, increased extracellular  $K^+$  is known to enhance  $I_{Kr}$  (13, 21)



# DIFFUSION



This appendix gives greater detail about the ionic movement theories, and electric theory properties generally, of the modelling of electrically active cells—note that this applies equally well to both cardiac cells and to neurons.

## A.1 Simple Diffusion

By simple diffusion, there is a net movement of particles from a region of high concentration to a region of low diffusion with simple thermal movement. This movement is according to Fick's Law,

$$F_X = -D \frac{\partial C_X}{\partial x}, \quad (\text{A.1})$$

where  $F_X$  and  $C_X$  represent the flux and concentration of particle  $X$  respectively, and  $D$  represents the diffusion coefficient. It should be noted that this represents *net* diffusion: there will be movement of particles in both directions. For circumstances where  $D$  is constant, this solves to produce

$$F_X = P(C_{X,o} - C_{X,i}), \quad (\text{A.2})$$

where  $P$  represents the permeability of the membrane, and is equivalent to  $D/d$ , where  $d$  represents the thickness of the membrane.  $C_{X,o}$  and  $C_{X,i}$  represent the extracellular and intracellular concentrations of  $X$ , respectively; thus  $F_X$  in this form describes flux from

the extra- to the intracellular space. It can be noted that for substances that diffuse through the lipid phase of the membrane, the permeability also depends on the oil/water partition coefficient  $\beta$ , according to  $P = \beta D/d$ .

## A.2 Facilitated Diffusion, Michaelis-Menten Kinetics

While Fick's Law can describe the movement of small, uncharged particles and some ions across a membrane very well, it does not serve particularly well for large molecules or charged substances. While ions can move across the membrane via membrane proteins such as channels and exchangers, some large molecules such as amino acids and glucose are large enough that pore-based channels would have no selectivity over what moves through them. Thus, they instead make use of *carrier-mediated diffusion*, also called *facilitated diffusion*, where the molecule binds to a transmembrane protein and causes a conformational change that results in the molecule being translocated across the membrane.

This mechanism obeys Michaelis-Menten kinetics, and can be viewed as a catalysed reaction, where the reaction is not a chemical one, but rather a translation of substance across the membrane.

Briefly, Michaelis-Menten kinetics are used to describe a two-stage reaction, the first stage being reversible, the second stage irreversible:



The above expression uses  $X_o$  and  $X_i$  to represent the extracellular and intracellular molecule respectively, and  $C$  the carrier;  $CX$  represents the moment when the molecule and the carrier combine for the transport process. It thus proposes that there is a reversible reaction between the extracellular molecule and the carrier, and that the transport process itself is irreversible. By certain assumptions, including that the number of

extracellular molecules is far greater than the number of carriers, the rate of this process can be estimated to be

$$v = \frac{dX_o}{dt} = v_{\max} \frac{[X_o]}{K_m + [X_o]}, \quad (\text{A.3})$$

where  $v$  represents the velocity of the reaction (*i.e.*, the rate of translocation of X),  $v_{\max}$  represents the maximum velocity at which the translocation can take place,  $[X_o]$  the concentration of X outside the cell,  $K_m$  represents the so-called Michaelis-Menten constant, which in turn represents the concentration at which the half-maximum speed occurs. It can be noted that  $v_{\max}$  is equal to the rate of the final step of the reaction.

Facilitated diffusion shows saturation (the point at which increasing the extracellular concentration further does not lead to an increase in flux), competitive and non-competitive inhibition, stereo-specificity and a relatively slow turnover.

## A.3 Electrodiffusion

This section deals with the form of transportation that is of most interest for this thesis: the passive movement of charged substances (ions) in the presences of an electrochemical gradient. It should be noted that the content in this section, while being in the appendix, is nonetheless vital for almost all mathematical models of electrically active cellular activity.

### A.3.1 The Nernst Equation

A key concept is that of the *Nernst Potential*, derived using the Nernst Equation, which describes the potential difference that is required to oppose the net flow of an ionic species against a specified concentration gradient. The equation shall here be derived in full using statistical mechanics.

Initially, recall that the probability of a system being in a particular state  $\alpha$  is given by

$$P(\alpha) = \frac{1}{Z} e^{-\beta E_\alpha}; \quad Z = \sum_i e^{\beta E_i}, \quad (\text{A.4})$$

where  $E_i$  is the energy of state  $i$ , and  $\beta = k_B T$ , with  $T$  being the temperature of the system.

For a large number of molecules,  $[A] \propto P(A)$ . Furthermore, if we consider the diffusion of ions from one location to another to be a reversible reaction according to  $A \xrightleftharpoons[k_2]{k_1} B$ , by applying the law of mass action ( $F_{A \rightarrow B} \propto [A]$ ), at steady state we achieve the following equation, which can be manipulated accordingly:

$$k_1[A] = k_2[B] \quad (\text{A.5})$$

$$\frac{[A]}{[B]} = \frac{k_2}{k_1} \quad (\text{A.6})$$

$$= \frac{\frac{1}{Z} e^{-\beta E_A}}{\frac{1}{Z} e^{-\beta E_B}} \quad (\text{A.7})$$

$$= e^{-\beta(E_A - E_B)} \quad (\text{A.8})$$

$$\Delta E = k_B T \ln \frac{[B]}{[A]} \quad (\text{A.9})$$

At this stage, the electric gradient is introduced to the equation as the reason for the energy difference that maintains the steady state, with  $\Delta E = zqV$ , where  $z$  is the valence of the ionic species being considered,  $q_e$  is the charge (in this case equal to the charge of an electron, *i.e.*, the charge of a singly ionised ion), and  $V$  is the potential difference.

$$zq_e V = k_B T \ln \frac{[B]}{[A]} \quad (\text{A.10})$$

$$V = \frac{k_B T}{zq_e} \ln \frac{[B]}{[A]} \quad (\text{A.11})$$

$$= \frac{RT}{zF} \ln \frac{[B]}{[A]} \quad (\text{A.12})$$

$$(\text{A.13})$$

Equations A.11 and A.12 are equivalent, the only difference being the constants used in the expression. Eq. A.12 is the more common formulation, using the gas constant  $R$  and the Faraday constant  $F$  in place of the Boltzmann constant  $k_B$  and the electron charge  $q_e$  respectively. The Nernst potential is, therefore, the potential difference that must be applied to maintain a specified concentration gradient, and is given by either equation.

# Bibliography

---

- [1] Bezanilla, F. (2000). The voltage sensor in voltage-dependent ion channels. *Physiological Reviews*, 80(2):555–92.
- [2] Carmeliet, E. (2006). Repolarization Reserve in Cardiac Cells. *Journal of Medical and Biological Engineering*, 26(3):97–105.
- [3] Carmeliet, E. and Vereecke, J. (2002). *Cardiac Cellular Electrophysiology*. Springer.
- [4] Cleemann, L., Wang, W., and Morad, M. (1998). Two-dimensional confocal images of organization, density, and gating of focal  $\text{Ca}^{2+}$  release sites in rat cardiac myocytes. *Proceedings of the National Academy of Sciences of the United States of America*, 95(18):10984–9.
- [5] Franzini-Armstrong, C., Protasi, F., and Tijskens, P. (2005). The assembly of calcium release units in cardiac muscle. *Annals of the New York Academy of Sciences*, 1047:76–85.
- [6] Greenstein, J. L. and Winslow, R. L. (2002). An integrative model of the cardiac ventricular myocyte incorporating local control of  $\text{Ca}^{2+}$  release. *Biophysical Journal*, 83(6):2918–45.
- [7] Haverkamp, W., Breithardt, G., Camm, a. J., Janse, M. J., Rosen, M. R., Antzelevitch, C., Escande, D., Franz, M., Malik, M., Moss, A., and Shah, R. (2000). The potential for QT prolongation and pro-arrhythmia by non-anti-arrhythmic drugs: clinical and regulatory implications. Report on a Policy Conference of the European Society of Cardiology. *Cardiovascular research*, 47(2):219–33.
- [8] Hodgkin, A. L. and Huxley, A. F. (1952). A quantitative description of membrane current and its application to conduction and excitation in nerve. *The Journal of Physiology*, 117:500–544.
- [9] Jost, N., Virág, L., Bitay, M., Takács, J., Lengyel, C., Biliczki, P., Nagy, Z., Bogáts, G., Lathrop, D. a., Papp, J. G., and Varró, A. (2005). Restricting excessive cardiac action potential and QT prolongation: a vital role for IKs in human ventricular muscle. *Circulation*, 112(10):1392–9.
- [10] Lengyel, C., Iost, N., Virág, L., Varró, A., Lathrop, D. A., and Papp, J. G. (2001). Pharmacological block of the slow component of the outward delayed rectifier current ( $\text{I}(\text{K}_s)$ ) fails to lengthen rabbit ventricular muscle QT(c) and action potential duration. *British journal of pharmacology*, 132(1):101–10.
- [11] Roden, D. M. (1998). Taking the "idio" out of "idiosyncratic": predicting torsades de pointes. *Pacing and Clinical Electrophysiology : PACE*, 21(5):1029–34.
- [12] Roden, D. M., Balser, J. R., George, A. L., and Anderson, M. E. (2002). Cardiac ion channels. *Annual Review of Physiology*, 64:431–75.
- [13] Sanguinetti, M. C. and Jurkiewicz, N. K. (1992). Role of external  $\text{Ca}^{2+}$  and  $\text{K}^{+}$  in gating of cardiac delayed rectifier  $\text{K}^{+}$  currents. *Pflügers Archiv : European journal of physiology*, 420(2):180–6.

- 
- [14] Silva, J. and Rudy, Y. (2005). Subunit interaction determines IKs participation in cardiac repolarization and repolarization reserve. *Circulation*, 112(10):1384–91.
  - [15] Spector, P. S., Curran, M. E., Zou, A., Keating, M. T., and Sanguinetti, M. C. (1996). Fast inactivation causes rectification of the IKr channel. *The Journal of general physiology*, 107(5):611–9.
  - [16] Vandenberg, J. I., Walker, B. D., and Campbell, T. J. (2001). HERG K<sup>+</sup> channels: friend and foe. *Trends in pharmacological sciences*, 22(5):240–6.
  - [17] Varró, A. and Baczkó, I. (2011). Cardiac ventricular repolarization reserve: a principle for understanding drug-related proarrhythmic risk. *British journal of pharmacology*, 164(1):14–36.
  - [18] Varró, A., Baláti, B., Iost, N., Takács, J., Virág, L., Lathrop, D. A., Csaba, L., Tálosi, L., and Papp, J. G. (2000). The role of the delayed rectifier component IKs in dog ventricular muscle and Purkinje fibre repolarization. *The Journal of Physiology*, 523 Pt 1(2000):67–81.
  - [19] Virág, L., Acsai, K., Hála, O., Zaza, A., Bitay, M., Bogáts, G., Papp, J. G., and Varró, A. (2009). Self-augmentation of the lengthening of repolarization is related to the shape of the cardiac action potential: implications for reverse rate dependency. *British journal of pharmacology*, 156(7):1076–84.
  - [20] Xiao, L., Xiao, J., Luo, X., Lin, H., Wang, Z., and Nattel, S. (2008). Feedback remodeling of cardiac potassium current expression: a novel potential mechanism for control of repolarization reserve. *Circulation*, 118(10):983–92.
  - [21] Yang, T., Snyders, D. J., and Roden, D. M. (1997). Rapid inactivation determines the rectification and [K<sup>+</sup>]<sub>o</sub> dependence of the rapid component of the delayed rectifier K<sup>+</sup> current in cardiac cells. *Circulation research*, 80(6):782–9.